Thickness Shear Mode Vibrations in Silicon Bar Resonators

Hengky Chandrahalim, Dana Weinstein and Sunil A. Bhave
OxideMEMS Group, 102 Phillips Hall, Cornell University, Ithaca, NY 14853, USA

ABSTRACT

This paper demonstrates a dielectrically transduced high quality factor (Q) quarter-wave thickness shear silicon resonator. Dielectric transduction provides a κ^2 reduction in motional impedance relative to air-gap electrostatic transduction. The resonator is fabricated on the 1.8 µm thick device layer of a heavily doped SOI wafer with 68 nm thick silicon nitride thin-film on top. The quarter-wave thickness shear mode of the silicon bar resonator has a resonant frequency of 713 MHz, a motional impedance R_x of 10.5 kΩ and Q of 1,517 in air. After partial release, the bar resonates at 723 MHz, exhibiting a motional impedance R_x of 2.4 kΩ and Q of 4,400 in air. Additionally, by varying a tuning voltage between the resonator and silicon substrate from 50 V to 150 V across a 2.5 micron gap, approximately 5 MHz of frequency tuning is observed.

INTRODUCTION

MEMS resonators are promising replacements to conventional SAW, ceramic and quartz resonators in direct conversion transceivers and chip-scale atomic clocks, demonstrating high resonant frequencies and relatively high quality factors. Air-gap electrostatically transduced MEMS resonators have quality factors (Q) > 10,000 but are limited by their large motional impedance (R_x > 10 kΩ) [1]. Alternately, piezoelectric FBARs have small motional impedance (R_x < 10 Ω) but relatively low Q (~ 2000) [2].

One of the main applications of the thickness shear mode resonator is the chip scale atomic clock (CSAC) [3], which uses hyperfine frequency splitting of Rb^{87} to generate a long-term stable signal. However, the CSAC does not have good short-term stability. Traditionally, a 10 MHz crystal oscillator in conjunction with a mixer, PLL and VCO is used to provide short-term stability for CSACs. But these components require high power, motivating a MEMS resonator alternative to provide a short-term stable signal.

The thickness shear mode resonator is a good candidate for several reasons. Its high-Q mode has been proven successfully in quartz resonators. Furthermore, it has a high frequency and low motional impedance. The thickness shear mode resonator also exhibits a small range of frequency tuning capability which is useful for compensation of frequency shift due to fabrication errors.

Dielectric transduction is achieved here by sandwiching a silicon nitride (κ~9) thin film between the silicon bar resonator and polysilicon electrodes. This enhances both the force density of the actuator as well as the sense capacitance, thereby improving the resonator's motional impedance by a factor of κ^2 [4].

QUARTER-WAVE THICKNESS SHEAR BAR RESONATOR

The asymmetric thickness shear mode is common in quartz resonators, excited by the application of an AC signal across electrodes on opposing faces of a quartz crystal [5]. Unlike the quartz thickness shear mode, the electrode configuration of the dielectrically transduced silicon bar induces a symmetric mode, as shown in Figure 1.

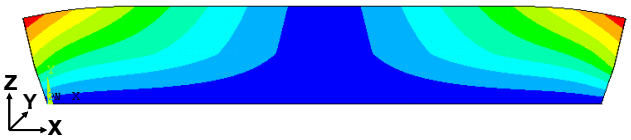

Figure 1. *X-displacement contour plot from Ansys simulation of the symmetric quarter-wave thickness shear mode.*

A one-dimensional thickness shear mode is derived for an unreleased silicon bar transduced by a thin dielectric film. The film, deposited on top of the bar, is sandwiched between the silicon bar and conducting top electrodes (Figure 2).

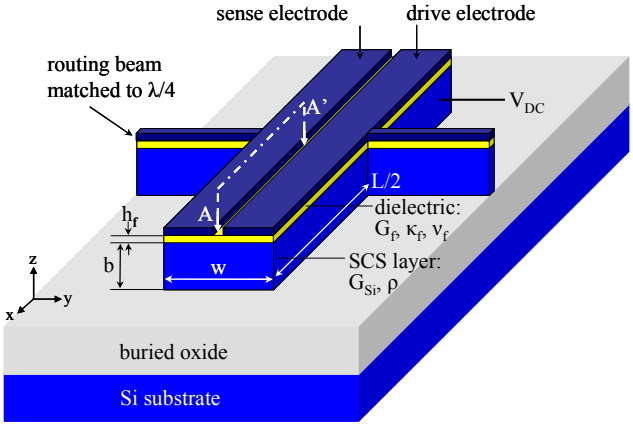

Figure 2. *Unreleased thickness shear bar diagram.*

The bottom face of the bar is fixed to an effectively infinite oxide layer, imposing a zero-displacement boundary condition at the base of the bar. In this configuration, the silicon bar is biased to a DC voltage V_{DC} while a small alternating voltage v_{AC} is applied to the top electrode. The voltage drop across the electrode-bar parallel plate capacitor induces a normal force on the dielectric film,

transferring to a lateral strain in the dielectric. Though the strain is in fact uniform in both lateral directions, we consider a long narrow bar, approximating a one dimensional model of the strain. This strain is distributed between the film and silicon bar, inducing a quarter-wave thickness shear resonant mode.

The lateral displacement u_x for the one-dimensional thickness shear mode is given by

$$u_x(x,z,t) = Ax\sin\left(\omega\left(\sqrt{\frac{\rho}{G}}\right)_{Si} z\right)e^{i\omega t} \quad (1)$$

for a resonant frequency of

$$\omega = \frac{\pi}{2b}\left(\sqrt{\frac{G}{\rho}}\right)_{Si} . \quad (2)$$

A voltage $V_{DC} + v_{AC}$ applied across the dielectric film generates a normal force

$$f_Z \approx -V_{DC}\frac{\kappa_f \varepsilon_0 wL}{2h_f^{\,2}} v_{AC} \quad (3)$$

for a bar of width w and length L, where κ_f and h_f are the relative permittivity and thickness of the dielectric film, respectively. Here, we make the approximation that $v_{AC} \ll V_{DC}$. The factor of 2 in the denominator arises from a configuration in which the drive electrode covers half the width of the bar, and the sense electrode occupies the other half.

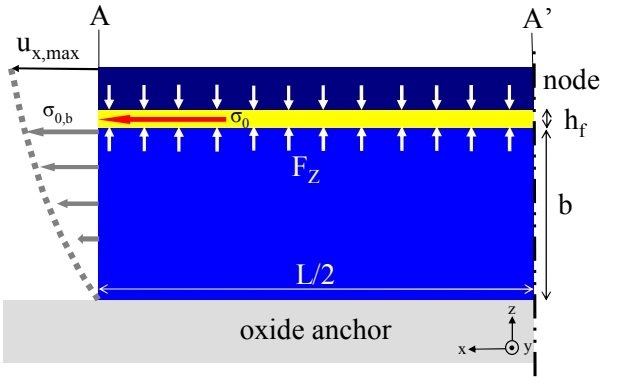

Figure 3. *2D cross-section schematic of the conversion of transverse electrostatic stress in the silicon nitride thin film to thickness shear mode in the half-length (A-A' in Figure 2) bar resonator. The approximation holds true for resonators with L >> w,b.*

The laterally transferred strain in the film is

$$\varepsilon_{y,f} = \nu_f \varepsilon_z = \frac{\nu_f f_z}{E_f wL} \quad (4)$$

and the lateral stress in the film is

$$\sigma_0 = E_f^{\,*}\varepsilon_{y,f} = \frac{\nu_f f_z}{(1-\nu_f)wL} \quad (5)$$

where E_f^* is the axial Young's modulus of the dielectric film. This initial lateral stress σ_0 functions like an effective residual stress in the film, consequently distributing itself in both film and bulk silicon, as illustrated in Figure 3. We assume that the shear stress in the silicon is distributed linearly through the bar due to the displacement boundary condition imposed by the oxide anchor. This yields a maximum shear stress in the silicon of

$$\sigma_{0,b} = \frac{G_{Si}h_f}{G_f h_f + \frac{1}{2}G_{Si}b}\sigma_0 \approx \frac{2h_f}{b}\sigma_0 \quad (6)$$

in the approximation that $h_f \ll b$. The maximum displacement of the bar can then be approximated as

$$u_{x,\max} = \frac{b}{G_{Si}}\sigma_{0,b} = \frac{\nu_f \kappa_f \varepsilon_0 V_{DC} v_{AC}}{(1-\nu_f)G_{Si}h_f} . \quad (7)$$

With the first-order determination of the quarter-wave thickness shear mode, we calculate the motional impedance R_X, inductance L_x, and capacitance C_x of the resonator. The change in the sensed capacitance over time is approximated as

$$\frac{\partial C}{\partial t} \approx \frac{Q\omega\kappa_f\varepsilon_0 wL}{2h_f^2}\Delta h_{\max} \quad . \quad (8)$$

The quality factor Q is introduced here to account for effective displacement amplification at resonance. The film is laterally expanded and contracted as the bar resonates, causing the thickness of the film to change with a Poisson efficiency factor. The maximum change in the film thickness is given by $\Delta h_{max} = \nu_f u_{x,max}$. The output current is

$$I_{OUT} = V_{DC}\frac{\partial C}{\partial t} = \frac{Q\pi(\nu_f\kappa_f\varepsilon_0 V_{DC})^2}{4(1-\nu_f)\sqrt{G_{Si}\rho}}\frac{wL}{h_f^{\,3}b}v_{AC} \quad (9)$$

giving a motional impedance of

$$R_X = \frac{v_{AC}}{I_{OUT}} = \frac{4\sqrt{G_{Si}\rho}}{Q\pi}\frac{(1-\nu_f)}{(\nu_f\kappa_f\varepsilon_0 V_{DC})^2}\frac{h_f^{\,3}b}{wL} \quad . \quad (10)$$

The effective mass for the thickness shear mode is

$$M_{eff} = \frac{\rho w}{L^2}\int x^2\sin^2(\omega\sqrt{\frac{\rho}{G_{Si}}}z)dxdz = \frac{1}{6}\rho wLb \quad (11)$$

and the effective spring constant is

$$K_{eff} = M_{eff}\omega^2 = \frac{\pi^2}{24}\frac{G_{Si}wL}{b} . \quad (12)$$

From equations 10-12, for $R_X \equiv \sqrt{(K_{eff}M_{eff})}/Q\eta^2$, the coupling constant η is

$$\eta^2 \approx \frac{(\pi wLV_{DC}\nu_f\kappa_f\varepsilon_0)^2}{24(1-\nu_f)h_f^{\,3}b} . \quad (13)$$

The motional capacitance $C_X \equiv \eta^2 / K_{eff}$ is

$$C_X = \frac{(V_{DC} \nu_f \kappa_f \varepsilon_0)^2}{(1-\nu_f) G_{Si}} \frac{wL}{h_f^3} \tag{14}$$

and the motional inductance $L_X \equiv M_{eff} / \eta^2$ is

$$L_X = \frac{4(1-\nu_f)\rho}{\pi^2 (V_{DC} \nu_f \kappa_f \varepsilon_0)^2} \frac{b^2 h_f^3}{wL}. \tag{15}$$

FABRICATION PROCESS

The resonator is fabricated in a 3-mask SOI process similar to [4]. A 68 nm low stress silicon nitride thin film is first deposited by LPCVD at 850°C on an n-type low resistivity SOI wafer with a 1.8 µm thick SCS device layer. The silicon nitride is patterned to open contact holes to bias the silicon resonator. A 120 nm layer of n-doped polysilicon is then deposited by LPCVD at 620°C, annealed at 1000°C for 40 minutes, and patterned to form the electrodes. This is followed by a deep reactive ion etch (DRIE) step to define the resonator into the silicon device layer (Figure 4(a)).

EXPERIMENTAL RESULTS

An unreleased 80 µm long by 40 µm wide bar resonator was characterized using a DesertCryo microwave probe station. The resonator body was grounded and a DC bias was applied to both the drive and sense electrodes with bias-Ts from MiniCircuits. Transmission measurements were performed using an Agilent 8753ES Network Analyzer and the quality factor and insertion loss were extracted from the measured data. The motional impedance of the resonator was determined from the insertion loss data after adjusting for the attenuation losses at the drive pad. The quarter-wave thickness shear vibration mode of the unreleased silicon resonator was measured with a resonant frequency of 713 MHz, an R_x of 10.5 kΩ and Q of 1,517 in air (Figure 4(b)).

It has previously been shown that quality factor improves with reduced anchor area. By performing a timed etch of the buried oxide in HF, the overall contact area between the oxide and bottom surface of the resonator was reduced to approximately 30 µm × 5 µm. This partially released bar had a resonant frequency of 723 MHz, R_x of 2.4 kΩ and Q of 4,400 in air (Figure 5). The large acoustic mismatch of the air gap reduces leakage of the shear standing wave into the anchor, thereby decreasing the quarter wavelength of the vibration mode. This explains the increased resonant frequency of the partially released bar relative to the unreleased bar.

The frequency response of the partially released bar gives a coupling factor $k_{em}^2 \equiv f_{zero}/f_{pole} - 1 \approx C_X/C_{FT}$ of $k_{em} = 0.03$. This is comparable to the coupling factor of quartz crystals [6].

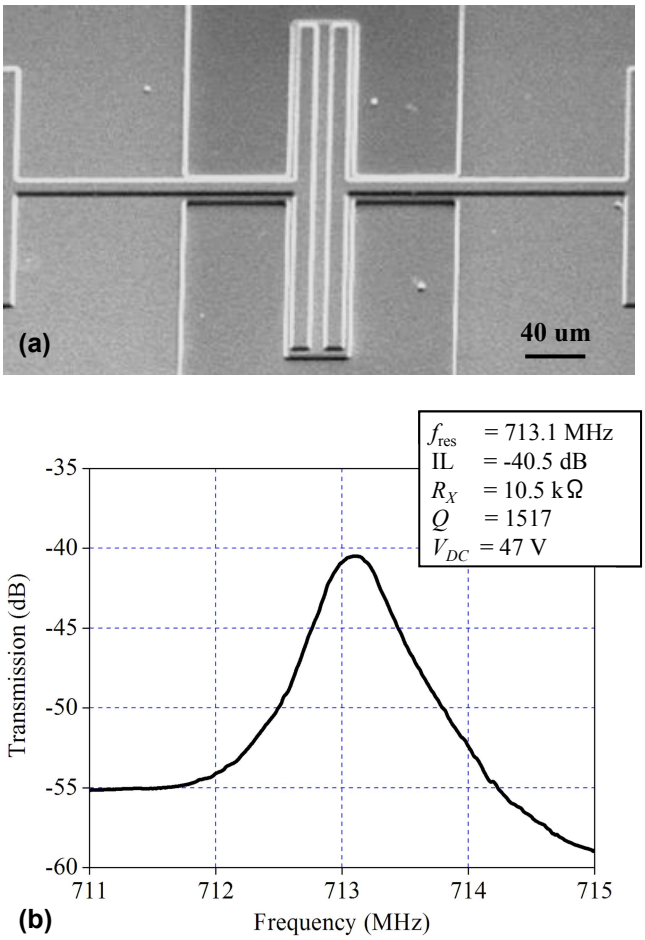

Figure 4. *(a) SEM of a silicon nitride-on-silicon unreleased bar resonator. (b) Measured transmission of the thickness shear mode of the unreleased resonator in air.*

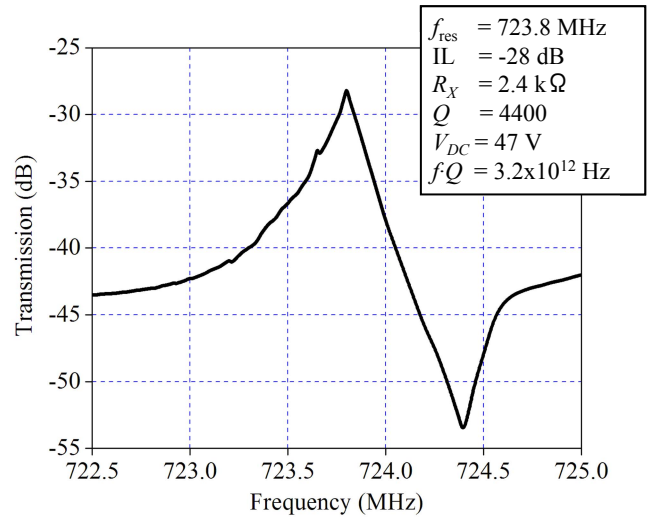

Figure 5. *Measured transmission of the shear mode of the partially released resonator in air. The reduction in anchor size increased the quality factor almost three-fold.*

ORTHOGONAL FREQUENCY TUNING

Previous attempts at frequency tuning forced a change in the effective stiffness of the resonator through deformations in the direction of resonant motion. However, the stiffness of high frequency resonators is very large in this direction, requiring considerable forces to tune the device. For example, a 1 GHz resonator has a stiffness on the order of 1 MN/m in the resonant direction. In the case of the partially released thickness shear bar resonator, the stiffness orthogonal to the resonant motion (z-direction) is very low. A static flexure of the bar as shown in Figure 6(a) reduces the effective shear stiffness. Varying the tuning voltage from 50 V to 150 V results in a 5 MHz change in resonant frequency with negligible degradation in quality factor (Figure 6(b)).

The high tuning voltages can be reduced significantly by decreasing the buried oxide thickness. Furthermore, scaling to higher frequencies will increase the tuning range, as the bar stiffness in the direction of tuning is proportional to b^3. This frequency tuning capability demonstrated by the thickness shear bar is highly beneficial for frequency shift compensation due to fabrication errors.

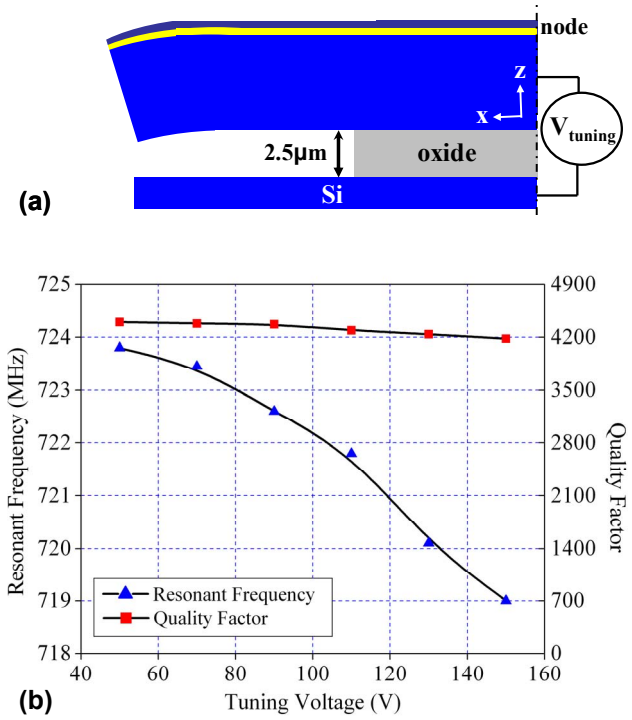

Figure 6. *(a) Tuning schematic for the partially released bar resonator. (b) Resonant frequency and quality factor vs. tuning voltage V_{tuning} of the bar resonator. A tuning range of about 5 MHz is observed with little reduction in Q.*

CONCLUSIONS

The partially released quarter-wave thickness shear bar resonator's *f-Q* product of 3.2×10^{12} Hz is within a factor of five of the *f-Q* product for quartz resonators [5]. Moreover, the 2.4 kΩ motional impedance of this resonator is the lowest motional impedance reported to date for any silicon-based VHF MEMS resonator design.

Thickness shear mode resonators using dielectric transduction achieve high frequencies with greatly improved motional impedance. The lateral electrode design causes a Poisson ratio inefficiency in the transfer of vertical strain into lateral strain. However, this transfer is necessary to induce a shear resonance. Furthermore, this configuration allows for a large electrode area, significantly decreasing the resonator's motional impedance.

Future improvement of the resonator includes reduction of the silicon device thickness to achieve higher resonant frequencies and a thinner buried oxide layer to permit wider tuning at lower bias voltages.

AKNOWLEDGEMENTS

The authors wish to thank DARPA CSAC program, whose generous grant has made this research possible. We would also like to thank Shankar Radhakrishnan, Dong Yan, Lih Feng Cheow, Steven Tin and Cornell Nanofabrication Facility for resonator fabrication.

REFERENCES

[1] J. Wang, *et al*, "1.51-GHz Polydiamond micromechanical disk resonator with impedance-mismatched isolating support," *MEMS 2004*, pp. 641–644.

[2] R. C. Ruby, *et al*, "Thin film bulk wave acoustic resonators (FBAR) for wireless applications", *Ultrasonics Symposium 2001*, pp. 813 – 821.

[3] C.T.-C. Nguyen, *et al*, "Towards chip-scale atomic clocks," *ISSCC 2005*, pp. 84-85.

[4] S. A. Bhave and R. T. Howe, "Silicon nitride-on-silicon bar resonator using internal dielectric transduction," *Transducers 2005*, pp. 2139-2142.

[5] F.P. Stratton, *et al*, "A MEMS-based quartz resonator technology for GHz applications," *Frequency Control Symposium 2004*, pp. 27-34.

[6] T. Mattila, *et al*, "Micromechanical bulk acoustic wave resonator," *Ultrasonics Symposium 2002*, pp. 945-948.